fishes

MDPI

Article

Transcriptome Profiling Revealed Basis for Growth Heterosis in Hybrid Tilapia (*Oreochromis niloticus* ♀× *O. aureus* ♂)

Jinglin Zhu [1,2], Zhiying Zou [2], Dayu Li [2], Wei Xiao [2], Jie Yu [2], Binglin Chen [2], Liangyi Xue [1,*] and Hong Yang [2,*]

[1] School of Marine Sciences, Ningbo University, Ningbo 315211, China; zhujinglin@ffrc.cn
[2] Key Laboratory of Freshwater Fisheries and Germplasm Resources Utilization, Ministry of Agriculture and Rural Affairs, Freshwater Fisheries Research Center, Chinese Academy of Fishery Sciences, Wuxi 214081, China; zouzhiying@ffrc.cn (Z.Z.); lidayu@ffrc.cn (D.L.); xiaowei@ffrc.cn (W.X.); yujie@ffrc.cn (J.Y.); chenbinglin@ffrc.cn (B.C.)
* Correspondence: xueliangyi@nbu.edu.cn (L.X.); yanghong@ffrc.cn (H.Y.)

Abstract: Hybrid tilapia were produced from hybridization of Nile tilapia (*Oreochromis niloticus*) and blue tilapia (*O. aureus*). Comparative transcriptome analysis was carried out on the liver of hybrid tilapia and their parents by RNA sequencing. A total of 2319 differentially expressed genes (DEGs) were identified. Trend co-expression analysis showed that non-additive gene expression accounted for 67.1% of all DEGs. Gene Ontology and KEGG enrichment analyses classified the respective DEGs. Gene functional enrichment analysis indicated that most up-regulated genes, such as *FASN*, *ACSL*1, *ACSL*3, *ACSL*6, *ACACA*, *ELOVL*6, *G6PD*, *ENO*1, *GATM*, and *ME*3, were involved in metabolism, including fatty acid biosynthesis, unsaturated fatty acid biosynthesis, glycolysis, pentose phosphate pathway, amino acid metabolism, pyruvate metabolism, and the tricarboxylic acid cycle. The expression levels of a gene related to ribosomal biosynthesis in eukaryotes, *GSH-Px*, and those associated with heat shock proteins (HSPs), such as *HSPA5* and *HSP70*, were significantly down-regulated compared with the parent tilapia lineages. The results revealed that the metabolic pathway in hybrid tilapia was up-regulated, with significantly improved fatty acid metabolism and carbon metabolism, whereas ribosome biosynthesis in eukaryotes and basal defense response were significantly down-regulated. These findings provide new insights into our understanding of growth heterosis in hybrid tilapia.

Keywords: hybrid tilapia (*Oreochromis niloticus* ♀× *O. aureus* ♂); transcriptome; growth-related genes; heterosis; fatty acid metabolism; carbon metabolism

Citation: Zhu, J.; Zou, Z.; Li, D.; Xiao, W.; Yu, J.; Chen, B.; Xue, L.; Yang, H. Transcriptome Profiling Revealed Basis for Growth Heterosis in Hybrid Tilapia (*Oreochromis niloticus* ♀× *O. aureus* ♂). *Fishes* **2022**, *7*, 43. https://doi.org/10.3390/fishes7010043

Academic Editor: Eric Hallerman

Received: 30 December 2021
Accepted: 7 February 2022
Published: 10 February 2022

1. Introduction

Heterosis, or hybrid vigor, refers to the superior performance of F_1 progeny compared with their homozygous parents [1]. This phenomenon has been widely exploited by aquaculture breeders for decades [2], such as in crucian carp (*Carassius auratus* red var.) [3], Pacific oyster (*Crassostrea gigas*) [4,5], and scallop (*Patinopecten yessoensis* ♀× *P. caurinus* ♂) [6]. Many hypotheses on the genetic mechanism of heterosis have been proposed, including the dominance hypothesis, over-dominance hypothesis, and epistasis hypothesis [7]. However, these genetic models were limited in their ability to explain the molecular bases of heterosis. Studies in transcriptomics, proteomics, metabolism, and epigenomics have provided new insights into parental genomic interactions, leading to regulatory and network changes and heterosis [1,8,9]. Recently, the differentially expressed genes (DEGs) and pathways related to heterosis have been identified through the transcriptome profiles analysis in aquatic species, such as hybrid grouper (*Epinephelus fuscogutatus* ♀× *E. lanceolatus* ♂) [10,11], hybrid pufferfish (*Takifugu obscurus* ♀× *T. rubripes* ♂) [12], hybrid tambacu (*Colossoma macropomum* ♀× *Piaractus mesopotamicus* ♂) [13], hybrid tilapia (*Oreochromis niloticus* ♀× *O. aureus* ♂) [14,15], hybrid carp (*Hypophthalmichthys nobilis* ♀× *H. molitrix* ♂) [16], hybrid seabream

(*Acanthopagrus schlegelii* ♂× *Pagrus major* ♀) [17], hybrid cypriniformes [*Megalobrama amblycephala* ♀× (*M. amblycephala* ♀× *Culter alburnus* ♂) ♂] [18], hybrid Chinese soft-shelled turtle (*Pelodiscus sinensis* Japanese strain ♀× *P.sinensis* Qingxi black turtle ♂) [19], sea cucumber (Chinese *Apostichopus japonicus* ♀× Russian *A. japonicus* ♂) [20], and hybrid abalone (*Haliotis gigantea* ♀× *H. discus* hannai ♂) [21]. These works could help us to further understand the molecular mechanism of the heterosis in various aquatic species.

China is the largest producer of tilapia with a production about 1.65 million tons in 2020 [22]. Crossbreeding is a common strategy used for genetic improvement within tilapia species [23,24]. Hybrid tilapia, produced from the hybridization of maternal *O. niloticus* and paternal *O. aureus*, are popular due to the high male percentage, which contributed significantly to the total tilapia production in China [24]. Hybrid tilapia shows a faster growth rate when compared to its parents [14]. However, the molecular bases are not well understood. Some authors have highlighted anthropogenic effects [25,26]. Theoretically, no new genes are produced in the F_1 hybrid, so heterosis is likely caused by differences resulting from qualitative or quantitative modifications of gene expression [27]. Gene expression patterns can be divided into either additive or non-additive expression on the basis of differential expression in the hybrids compared with the parents. Non-additive genes, which are genes in the hybrids that show significantly different expression from the mid-parent value, have been suggested to be associated with heterosis [28–30]. Recent studies of hybrid yellow catfish Huangyou-1 (*Pelteobagrus fulvidraco* ♀× *P.vachelli* ♂) [8] and hybrid abalone (*Haliotis diversicolor* Taiwan genotype ♀× *H. diversicolor* Japan genotype ♂) [31] have also focused on the non-additively expressed genes to characterize gene regulation and its underlying mechanisms.

In order to reveal the mechanisms underlying the heterosis in hybrid tilapia (*O. niloticus* ♀× *O. aureus* ♂), comparative transcriptome analysis was carried out between hybrid tilapia and its parental lines. It is hypothesized that the non-additive modes of gene expression are vital to realization of heterosis generation in hybrid tilapia.

2. Materials and Methods

2.1. Sample Collection and Preparation

Experimental fish used in the study were cultivated at the Tilapia Genetic Breeding Center of the Ministry of Agriculture and Rural Affairs, Wuxi, China. Two tilapia varieties, "Egypt strain" *O. niloticus* (N for short) and "Xia'ao strain" *O. aureus* (A for short), were both from inbred lines produced through several generations of sibling mating; the sterile hybrid tilapia (N ♀× A ♂, NA for short) were the F_1 offspring of these two lines. All individual fish were cultured in three open 0.067-ha pools under the same conditions. Then one-hundred healthy fish of each line were randomly selected and kept in a recirculating system (360-L tanks with circulating aerated water) to acclimate for 14 days. Water quality was monitored daily and maintained as follows: temperature, 29.0 ± 1 °C; pH, 7.6–7.8; dissolved oxygen (DO), >5.0 mg/L. The fish were fed a commercial feed twice a day (8:00 and 16:00). No tilapia died during the acclimation.

At the end of the trial, after 24 h of starvation, 30 males of each line were randomly selected for measure. Hybrid tilapia had a body mass of 63.65 ± 4.84 g. The body mass of *O. niloticus* was 59.65 ± 4.59 g, whereas that of *O. aureus* was 60.71 ± 5.63 g, which were lighter than that of hybrid tilapia ($p < 0.05$). Three males per line with a normal appearance and good vitality were deeply anesthetized with 100 mg/L MS-222 (Sigma-Aldrich, St. Louis, MO, USA) before dissection. There were no skin lesions before tissues were collected. The liver tissues excised from fish were snap-frozen in liquid nitrogen and then stored at −80 °C for subsequent RNA isolation. The protocols used meet the Zhejiang Laboratory Animal Management guidelines (000014349/2017-768264) established by the government of Zhejiang province on the use and care of animals.

2.2. RNA Extraction, Library Construction, and Transcriptome Sequencing

Total RNA was extracted using TRIzol™ Reagent (Invitrogen, Carlsbad, CA, USA) according to the manufacturer's protocol. Three independent biological replicates were performed for each tilapia line. RNA concentration was measured using a NanoDrop™ 2000 (Thermo Scientific, Waltham, MA, USA). RNA integrity was assessed using the RNA 6000 Nano Assay Kit of the Agilent 2100 Bioanalyzer system (Agilent Technologies, Santa Clara, CA, USA).

For RNA library preparation, the RNA of each individual from each tilapia line was diluted to the same concentration with RNase-free water. The three RNA samples from each line were equally mixed together (1 μg RNA from each sample) to obtain three groups. In order to select cDNA fragments of preferentially 240 bp in length, the library fragments were purified with the AMPure XP system (Beckman Coulter, Beverly, MA, USA). Sequencing libraries were generated using the NEBNext® Ultra™ RNA Library Prep Kit for Illumina® (NEB, Ipswich, MA, USA) following manufacturer's recommendations and index codes were added to attribute sequences to each sample. The clustering of the index-coded samples was performed on a cBot Cluster Generation System using TruSeq PE Cluster Kit v4-cBot-HS (Illumina, San Diego, CA, USA). After cluster generation, the library preparations were sequenced on an Illumina HiSeq X Ten platform by Biomarker Technologies (Beijing, China). Paired-end reads were generated, each about 150 bp long.

2.3. Data Filtering, Comparative Analysis, and Gene Functional Annotation

Raw reads in FASTQ format were first processed through in-house Perl scripts. In this step, clean reads were obtained by removing reads containing adapters, reads containing poly-N, and low-quality reads from the raw data. Simultaneously, Q_{30}, GC content, and sequence duplication level of the clean data were calculated. The clean data were submitted to the National Center for Biotechnology Information (NCBI), deposited in the Sequence Read Archive (SRA) under BioProject PRJNA792260(SUB10844155), with the accession numbers SRR17399951, SRR17399952 and SRR17399953.

These clean reads were then mapped to the reference genome sequence (https://www.ncbi.nlm.nih.gov/genome/197?genome_assembly_id=28435, accessed on 18 March 2015). Only reads with a perfect match or one mismatch were further analyzed and annotated based on the reference genome. The TopHat2 tool was used to map the reads to the reference genome [32].

Gene function was annotated based on the following databases: NCBI non-redundant protein sequences, NCBI non-redundant nucleotide sequences, Pfam (Protein family), Clusters of Orthologous Groups of proteins, Swiss-Prot, KEGG Ortholog, and Gene Ontology (GO).

2.4. Quantification of Gene Expression Levels and Differential Expression Analysis

Gene expression levels were estimated by fragments per kilobase of transcript per million fragments mapped (FPKM). Differential expression analysis between hybrid tilapia and their parents was performed using the EBSeq R package [33]. The resulting p values were adjusted using the Benjamini and Hochberg approach to control the false discovery rate. Genes showing a false discovery rate < 0.01 and a $|\log2(\text{fold-change})| \geq 1$ were considered significant differentially expressed genes (DEGs). The difference in gene expression level between two tilapia lines was displayed by volcano plot. The DEGs were subjected to trend co-expression analysis according to *K*-means clustering and were classified into five patterns (Figure 1): over-dominant, high-parent dominant, low-parent dominant, under-dominant, and additive. These analyses were performed using BMKCloud (www.biocloud.net, accessed on 7 March 2020).

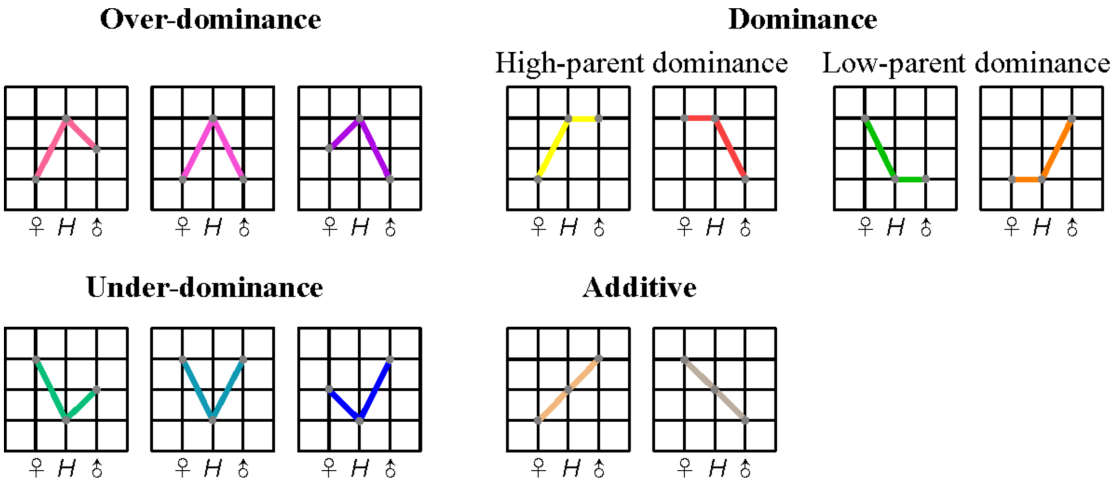

Figure 1. The possible different gene expression patterns in hybrid tilapia relative to their parents. Note: H refers to hybrid tilapia, ♀refers to *O. niloticus*, ♂refers to *O. aureus*.

2.5. GO and KEGG Enrichment Analysis of DEGs

GO enrichment analysis of DEGs was implemented in the goseq R package using the Wallenius non-central hyper-geometric distribution [34]. KOBAS 2.0 (Peking University, Beijing, China) was used to test the statistical enrichment of DEGs in KEGG pathways [35]. GO terms and KEGG pathways showing a corrected $p \leq 0.05$ were considered significantly enriched. Hierarchical cluster analyses of DEGs were constructed. The R program was used to depict the heat maps for gene clustering.

2.6. Validation of RNA-Seq Data by Quantitative Real-Time PCR (qRT-PCR)

Sixteen growth-related genes were selected for RNA-Seq data validation using qRT-PCR. After transcriptome sequencing, the remaining nine RNA samples were returned by mail on dry ice; then, 1 µg of total RNA was converted to cDNA by a PrimeScript™ RT reverse transcription kit (TaKaRa, Dalian, China) according to the manufacturer's instructions. Primers were designed using Primer Premier 5 and were synthesized at Biotech Bioengineering Co. (Shanghai, China) (Table 1). QRT-PCR validated the DEGs between hybrid tilapia (NA) and their maternal *O. niloticus* (N) and paternal *O. aureus* (A).

Table 1. Genes and PCR primer sequences used for quantitative real-time PCR.

Gene	Forward Primer Sequence (5′-3′)	Reverse Primer Sequence (5′-3′)
FASN	AAGCGGTTGATGTCCTCGTAAG	TGGCTGTAAGGCAGTCCGTCTC
ELOVL6	GCTGTGGTCACTCACCCTTGCT	CTGACTGTTTGAGCCCTTTCGT
ACACA	GGGAGTTCGGACAGCACCTAT	ATGACCCTGTTACCACCAAAGC
FADS2	CACTTGTTTCCAATGATGCCG	CCAGAGGTCCCCAGAGGTTTT
ELOVL5	CAGATCACGTTCCTGCACCTC	GGATGGCTGGAATGGCTGA
GATM	GCTGGGACGGACCTCTTTGT	GGGCGATCTGGGTTTGACA
SHMT	CCTTGACTATGCCCGCTTGA	GTGCGTCGTCGTGGTAACAAT
ME3	GAGGATGTGGTGCGGGAACT	CAGCTTTGCTGGTCGGGTT
ACS	GCCTCGTCATCAAGCACCAT	GGCCTCATCCCACCAAACAT
ALT	ACCCCTCGTACCCGCTCTAT	AACGCAAACAATCCTCCTTCAA
ENO1	TACCCAGTGGTGTCCATTGAGG	CGGAGCCAATCTGGTTGACTTT
NOG1	CGCATTCTCGCCGAACAGA	CGCGTAGTGGCTATCGTCCTT
NOP56	AAGCGGAGTCGGAGGAAGTAG	AGTCACAGGTGTTTCTGGGGTC
SNU13	CTGAGGAAGGGAGCCAACGA	AGCGGCAGGTGGAGGATGAT
IGF-2	ACGCAGAACAGCAGAATGAAGG	GCCGAGGCCATTTCCACTAC
GSH-Px	TGAGAAGTTTCTGGTGGGAAGG	TGCGTACTGTTCGAGCAGGTAT
β-actin	CCACACAGTGCCCATCTACGA	CCACGCTCTGTCAGGATCTTCA

The qRT-PCR assays were performed on a 7900HT Fast Real-Time PCR instrument (ABI, Waltham, MA, USA). The reaction system (20 µL) was: 10 µL 2×SYBR Green Real-time PCR Master Mix (Toyobo, Osaka, Japan), 1 µL cDNA template (5-fold dilution), 0.6 µL of each primer (10 µmol/L), and 7.8 µL ddH_2O. Optimized reactions were performed under the following conditions: 94 °C for 4 min, followed by 40 cycles of 94 °C for 15 s, 60 °C for 20 s, and 72 °C for 40 s. *β-actin* was used as an internal control in qRT-PCR. The relative expression levels of the target genes were calculated using the $2^{-\Delta\Delta Ct}$ approach [36].

2.7. Statistical Analysis

All qRT-PCR data were expressed as the mean ± standard error. Statistical significance of differences was determined using one-way ANOVA in SPSS 25.0 (IBM, Chicago, IL, USA). $p < 0.05$ was considered to indicate a statistically significant difference. Tukey's test was applied to detect significant differences ($p < 0.05$). Graphs were made with GraphPad Prism 8 (GraphPad Software, San Diego, CA, USA).

3. Results

3.1. Sequencing Data Statistics

After sequence quality control, a total of 19.54 Gb clean data were obtained, and the Q_{30} base percentage was above 90.20% (Supplementary Table S1). RNA-Seq obtained over 6.22 Gb of clean reads from each sample, and the average GC content was approximately 50%. The alignment efficiency ranged from 65.77% to 73.85% (Supplementary Table S2). A total of 1687 novel genes were discovered, of which 1546 were annotated.

3.2. Identification of Differentially Expressed Genes

A total of 2319 DEGs were identified, of which 956, 1119, and 1411 DEGs were found between *O. niloticus* and hybrid tilapia (N vs. NA), *O. aureus* and hybrid tilapia (A vs. NA), *O. niloticus* and *O. aureus* (N vs. A), respectively. In total, 466 genes were up-regulated and 490 genes were down-regulated in "N vs. NA", 507 genes were up-regulated and 612 genes were down-regulated in "A vs. NA", and 774 genes were up-regulated and 637 genes were down-regulated in "N vs. A" (Figure 2a). Volcano plots present the up- and down-regulated DEGs through pairwise comparisons (Supplementary Figure S1).

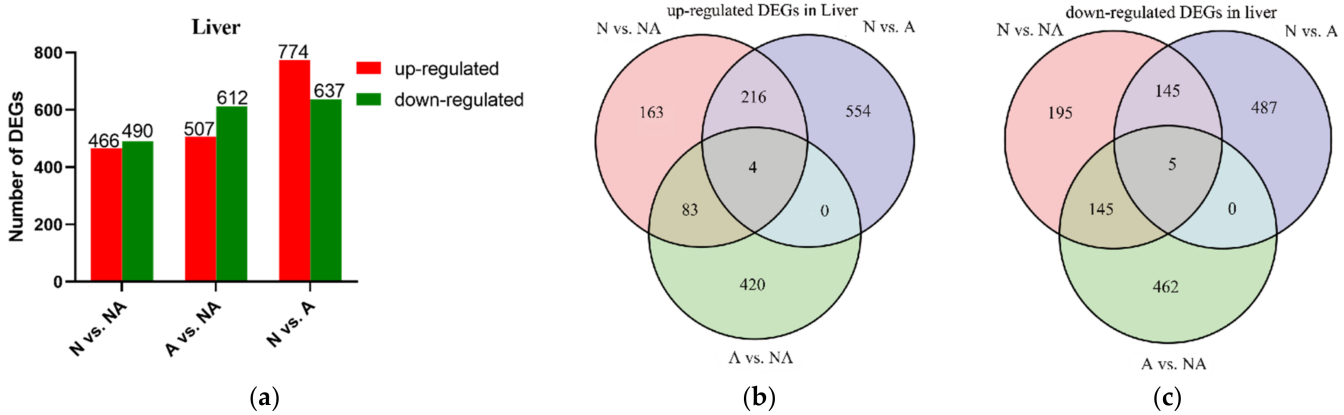

Figure 2. Number of DEGs in the three tilapia lines. (**a**) Total number of up- and down-regulated DEGs between hybrid tilapia (NA) and their maternal *O. niloticus* (N) and paternal *O. aureus* (A). (**b**) Venn diagram of up-regulated DEGs. (**c**) Venn diagram of down-regulated DEGs. Note: NA refers to hybrid tilapia, N refers to *O. niloticus*, A refers to *O. aureus*.

Of the 1440 up-regulated DEGs between the pure species (N and A) and hybrid (NA), 220 DEGs were also among the DEGs between N and A. In addition, 163 DEGs were specifically expressed in "N vs. NA" and 420 DEGs in "A vs. NA"; 4 DEGs were co-expressed in "N vs. NA", "A vs. NA", and "N vs. A"; and 83 overlapping DEGs were specifically found in "N vs. NA" and "A vs. NA". Therefore, a total of 666 unique

up-regulated DEGs were identified and further selected for GO annotation and KEGG enrichment analysis (Figure 2b). Similarly, a total of 802 unique down-regulated DEGs were identified and further selected for GO annotation and KEGG enrichment analysis (Figure 2c).

3.3. Trend Co-Expression Analysis of DEGs

The 2319 DEGs were categorized into 15 gene clusters (Figure 3). A large proportion of the genes (1556, 67.1%) showed non-additive gene expression in livers of hybrid tilapia. Of these 1556 genes, 482, 112, 455, and 507 exhibited overdominance, high-parent dominance, low-parent dominance, and under-dominance patterns, respectively. Additionally, 763 DEGs exhibited additive-type gene expression, which accounted for 32.9% of all DEGs.

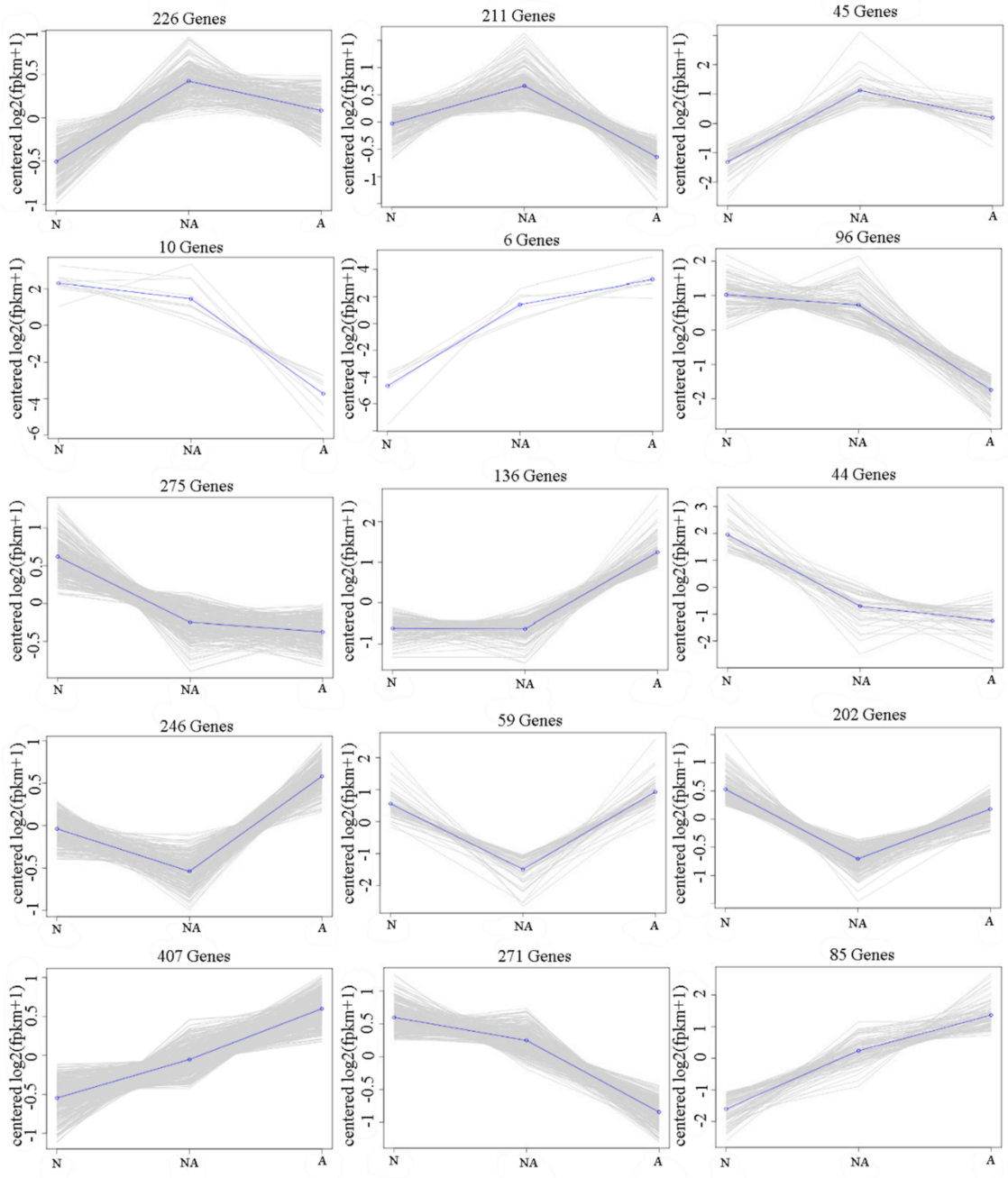

Figure 3. Trend co-expression analysis of DEGs between hybrid tilapia (NA) and their maternal *O. niloticus* (N) and paternal *O. aureus* (A).

3.4. GO and KEGG Enrichment Analysis of DEGs

Based on GO annotation, 389 of 666 up-regulated DEGs were enriched into 42 GO terms (Supplementary Figure S2). Under biological process, the DEGs were enriched in those associated with metabolic processes and single biological processes. In cellular components, the DEGs were enriched in cellular components and cells. In molecular function, the DEGs were enriched in catalytic activity and binding.

By KEGG analysis, the up-regulated DEGs were significantly enriched in metabolic pathway, including fatty acid metabolism, carbon metabolism, peroxisome, biosynthesis of unsaturated fatty acids, fatty acid biosynthesis, glycine, serine and threonine metabolism, pyruvate metabolism, biosynthesis of amino acids, and arginine and proline metabolism (Figure 4a).

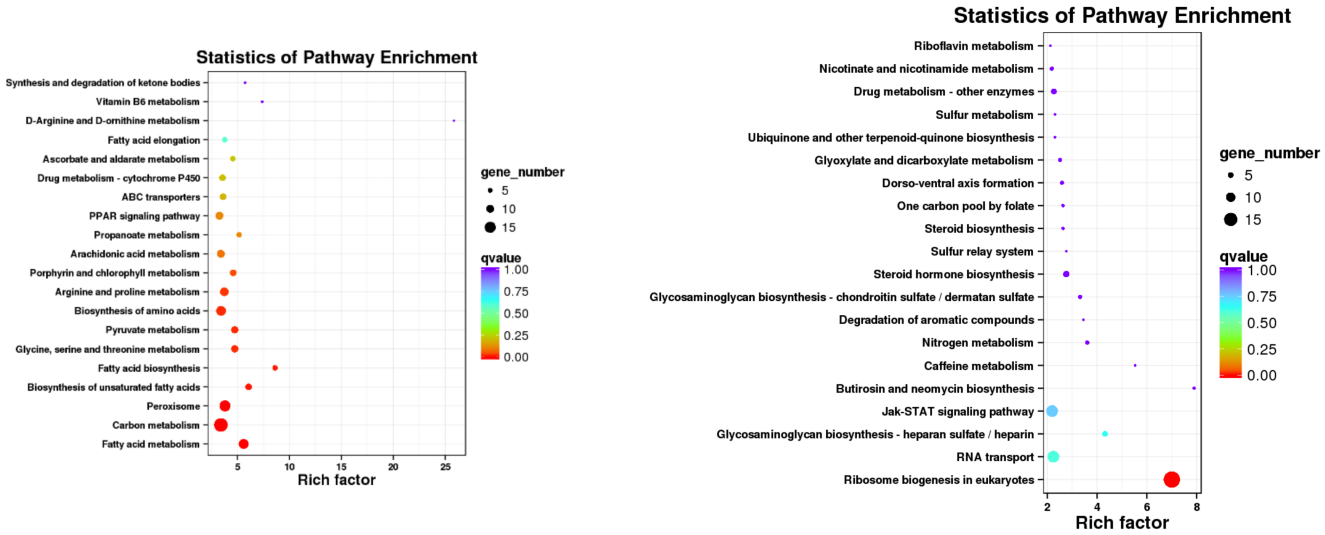

(**a**) (**b**)

Figure 4. KEGG pathway enrichment analysis of significantly up-regulated DEGs (**a**) and down-regulated (**b**) DEGs between *O. niloticus* or *O. aureus* and hybrid tilapia.

A total of 458 of the 802 down-regulated DEGs were enriched into 46 GO terms (Supplementary Figure S3). Under biological processes, the DEGs were enriched in cellular processes and metabolic processes. In cellular components, the DEGs were enriched in cellular fractions and cells. In molecular function, the DEGs were enriched in binding and catalytic activity. KEGG analysis showed that 802 down-regulated DEGs were significantly enriched in ribosome biogenesis in eukaryotes (Figure 4b).

3.5. Analysis of DEGs Potentially Related to Hybrid Tilapia Heterosis

Based on the GO and KEGG analysis, we selected 32 DEGs that may be most related to hybrid tilapia heterosis. The FPKM values of the DEGs for NA, N, and A are detailed in Table 2.

3.5.1. DEGs Related to Fatty Acid Metabolism

We found that five genes related to fatty acid biosynthesis, including fatty acid synthase (*FASN*), long-chain fatty acid-CoA ligase (*ACSL1, ACSL3, ACSL6*), and acetyl coenzyme A carboxylase (*ACACA*) of NA had higher FPKMs value than both N and A, and so were long-chain fatty acid elongase (*ELOVL5* and *ELOVL6*) and fatty acid desaturase (*FADS2*), involved in unsaturated fatty acid biosynthesis. The results provide further evidence that fatty acid metabolism enzyme genes were more active in hybrid tilapia.

Table 2. FPKMs referring to fatty acid metabolism, carbon metabolism, ribosome biogenesis in eukaryotes, and defense-related genes in three tilapia lines.

Function	Gene	ID	NA-FPKM	N-FPKM	A-FPKM
Fatty acid metabolism	*FASN*	gene:ENSONIG00000007292	982.98	354.62	76.84
	ELOVL5	gene:ENSONIG00000009696	3920	192.85	154.27
	ELOVL6	gene:ENSONIG00000001109	535.45	249.52	134.74
	ACSL6	gene:ENSONIG00000017218	29.69	13.55	17.75
	ACSL1	gene:ENSONIG00000017586	265	7.70	4.93
	ACSL3	gene:ENSONIG00000014644	0.77	0.13	0.09
	FADS2	gene:ENSONIG00000015532	410.86	216.16	89.65
Carbon metabolism	*ENO1*	gene:ENSONIG00000002418	89.38	31.23	24.72
	ME3	gene:ENSONIG00000000106	257.54	82.64	8.00
	ACS	gene:ENSONIG00000018471	205.65	86.71	15.60
	PFK1	gene:ENSONIG00000011877	23.28	10.96	12.04
	PSPH	gene:ENSONIG00000008118	10.72	4.49	1.79
	PSAT1	gene:ENSONIG00000016998	6.34	1.26	1.22
	GATM	gene:ENSONIG00000000198	412.59	29.92	66.46
	ACACA	gene:ENSONIG00000001922	265.98	89.27	42.66
	PGD	gene:ENSONIG00000002336	47.47	30.54	14.74
	GSPD-1	gene:ENSONIG00000017037	44.85	34.61	20.25
	G6PD	gene:ENSONIG00000000416	44.67	28.09	19.16
	PFKL	gene:ENSONIG00000009075	5.72	3.32	2.32
Defense-related genes	*HSPA5*	gene:ENSONIG00000002826	188.08	678.45	3833
	GSH-Px	gene:ENSONIG00000017717	84.06	218.45	2979
	PIM1	gene:ENSONIG00000000258	52.95	130.25	200.23
	HSP70	gene:ENSONIG00000005214	2.33	7.61	8.46
Ribosome biogenesis in eukaryotes	*SNU13*	gene:ENSONIG00000019849	12.13	34.88	32.03
	DKC1	gene:ENSONIG00000013889	10.35	29.10	23.45
	UTP5	gene:ENSONIG00000019540	3.80	12.45	14.62
	Nug1/2	gene:ENSONIG00000019335	2.57	13.09	16.23
	UTP15	gene:ENSONIG00000014323	2.51	7.15	7.78
	MPP10	gene:ENSONIG00000002999	1.29	5.41	4.33
	UTP4	gene:ENSONIG00000004191	1.27	5.00	4.66
	UTP14	gene:ENSONIG00000020563	1.14	3.82	5.42
	UTP10	gene:ENSONIG00000019095	0.66	2.04	1.66

3.5.2. Carbon Metabolism-Related DEGs

Carbon metabolism-related genes in liver, such as 6-phosphofructokinase-1 (*PFK1*) and enolase (*ENO1*) in the glycolytic pathway (EMP), glucose-6-phosphate dehydrogenase (*G6PD*) in the pentose phosphate pathway (PPP), malate dehydrogenase (*ME3*), and acetyl coenzyme A synthase (*ACS*) in the TCA cycle, were significantly up-regulated in hybrid tilapia compared with their parents. In addition, the key enzymes of the amino acid metabolic pathway, including glycine aminotransferase (*GATM*), glycine hydroxymethyltransferase (*SHMT*), phosphoserine phosphatase (*PSPH*), and phosphoserine aminotransferase 1 (*PSAT1*), were significantly increased in hybrid tilapia. Hierarchical cluster analysis of up-regulated DEGs is shown in Figure 5a.

3.5.3. Eukaryotic Biosynthesis and Defense-Related DEGs

The key enzymes of eukaryotic biosynthesis, *SNU13, DKC1, Nug1/2, MPP10, UTP4, UTP5, UTP14, UTP10,* and *UTP15,* were significantly down-regulated in hybrids compared with the parents. The antioxidant-related gene *GSH-Px* and HSP family genes (*HSPA5* and *HSP70*) were also significantly down-regulated. Hierarchical cluster analysis of down-regulated DEGs is shown in Figure 5b.

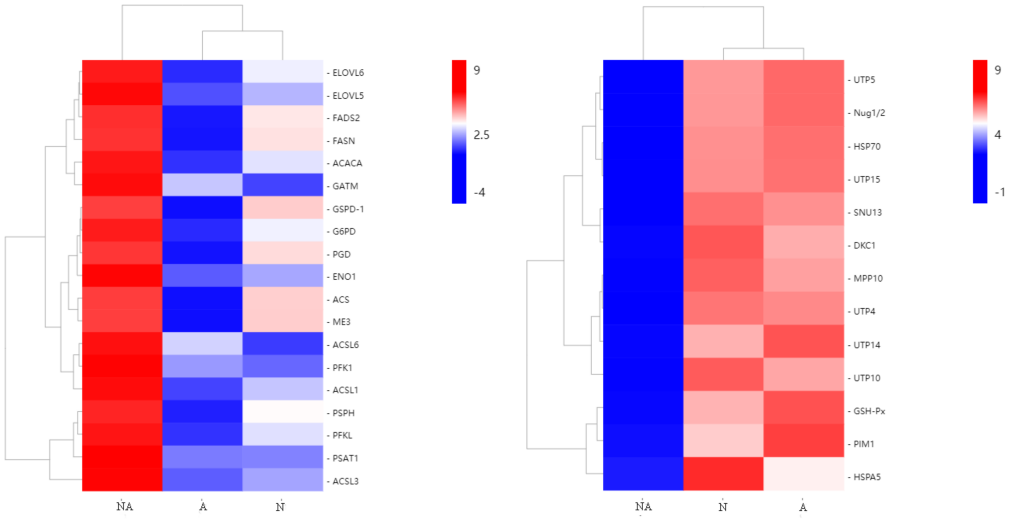

Figure 5. Hierarchical cluster analysis of up-regulated (**a**) and down-regulated (**b**) DEGs involved in heterosis. Note: The color key represents FPKM normalized log2-transformed counts in livers of three tilapia species. Changes in expression levels are shown using color scales with saturation at >two-fold changes. Red and blue gradients indicate an increase and decrease of DEGs, respectively.

3.6. Validation of RNA-Seq Data by qRT-PCR

As shown in Figure 6, the expression patterns of 16 DEGs detected by qRT-PCR were highly consistent with the data produced by RNA-Seq, which indicated that the sequencing results were reliable and accurate.

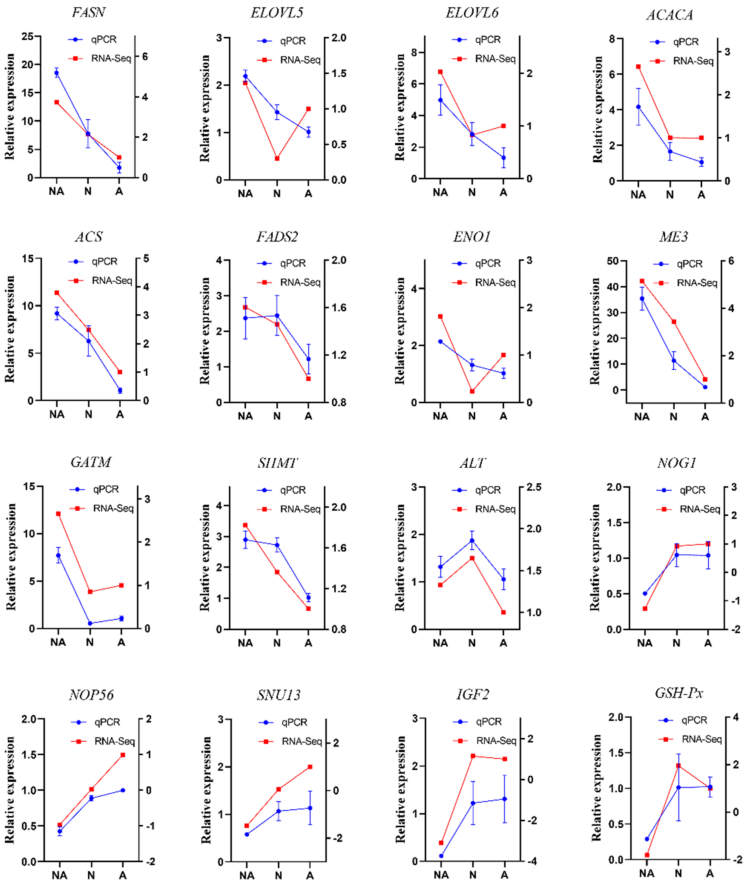

Figure 6. Validation of RNA-Seq data of sixteen DEGs by qRT-PCR.

4. Discussion

Heterosis has been widely exploited in aquaculture breeding [3–6]. Hybrid tilapia, the offspring of maternal *O. niloticus* and paternal *O. aureus*, has been demonstrated to have enhanced performance traits, such as faster growth rate, and better stress and disease tolerance [14,15]. However, the molecular mechanisms underlying this phenomenon remain elusive. Zhou et al. [14] and Zhong et al. [15] illustrated the concept of GH and IGF-1 expression superiority and its mechanism for promoting vigorous growth in hybrid tilapia, respectively. In the current study, we constructed RNA-seq libraries of the livers of hybrid tilapia and its parents, and detected some DEGs and pathways that may be responsible for heterosis. Subsequently, trend co-expression analysis showed that non-additive gene expression patterns were prevalent in the liver of hybrid tilapia. In the end, based on the function of these DEGs and their location in the pathway, an overview of the superior growth generation was produced (Figure 7).

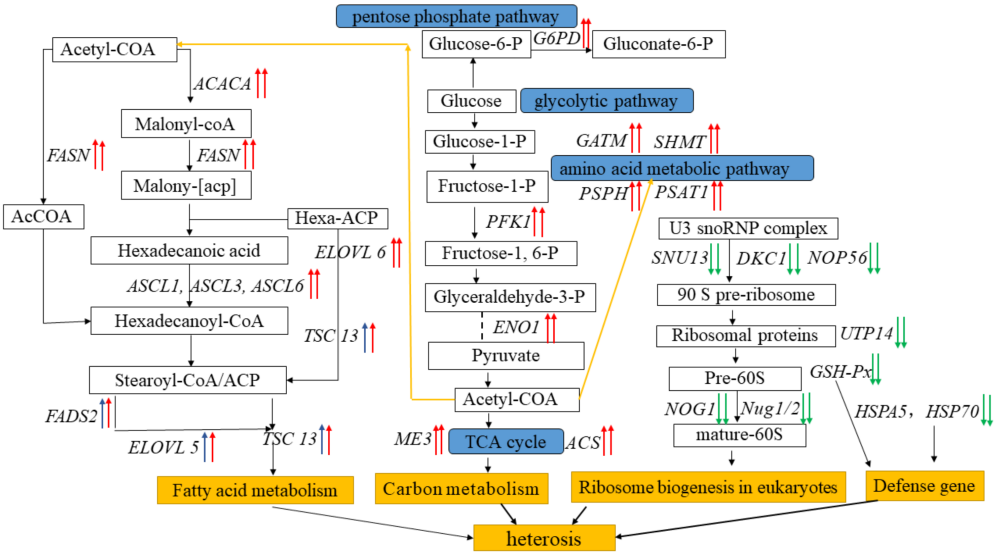

Figure 7. Overview of molecular mechanisms underlying the enhanced growth of hybrid tilapia. Note: Red arrows indicate a significant increase, blue arrows indicate non-significant increase, and green arrows indicate a significant decrease. The first arrow indicates the gene expression trend in hybrid tilapia (NA) compared with *O. niloticus* (N), and the second arrow indicates the gene expression trend in hybrid tilapia compared with *O. aureus* (A).

4.1. Analysis of Candidate DEGs Involved in Fatty Acid Metabolism

The levels of expression of numerous genes involved in the fatty acid metabolism pathway, such as *FASN*, *ELOVL5*, *ELOVL6*, *ACSL6*, *ACSL*1, *ACSL3*, and *FADS2*, were up-regulated in the livers of hybrid tilapia compared with the parental species. Fatty acid synthase (*FASN*) is an important rate-limiting enzyme that catalyzes the synthesis of fatty acids used for energy generation, extended with C2 units derived from the elongation substrate malonyl-CoA [37]. The biosynthesis of long-chain polyunsaturated fatty acids requires the concerted activities of fatty acyl desaturase (*FADS*) and elongase (*ELOVL*) [38]. Similarly, Zheng et al. [18] found significant up-regulation of *FAS*, *ELOVL*1, *ELOVL*5, and *ELOVL6* expression in a new backcross of *T. gigas* ♀× (*T. gigas* ♀× *Bleak* ♂) ♂, the growth advantage of this backcross may be related to the increased fatty acid synthesis. These up-regulated genes may lead to accelerated fatty acid synthesis and fatty acid metabolism.

4.2. Analysis of Candidate DEGs Involved in Carbon Metabolism

Carbon metabolism, which includes the EMP, PPP, and the TCA cycles, is very important for providing materials and energy for fish growth. Glycolysis plays a central role in the anabolism and catabolism of organisms [39], and provides intermediates for

other metabolic pathways, such as gluconeogenesis, fatty acid metabolism, biosynthesis of amino acids, and the TCA cycle [40,41]. Almost all glycolytic genes were up-regulated in hybrid grouper compared with their parents [11]. In this study, both *PFK1* and *ENO1* in the glycolysis pathway were up-regulated in hybrid tilapia. The TCA cycle is a crucial pathway for generating energy through oxidizing carbohydrates and fatty acids [42]. In the current study, significantly enriched DEGs encoding *ME3* and *ACS* were found in the TCA cycle. Additionally, the amino acid metabolic pathway genes *GATM*, *SHMT*, *PSPH*, and *PSAT1*, *G6PD* involved in PPP, were up-regulated in the F_1 hybrids. These findings indicated a dramatic change in efficiency of amino acid metabolism between F_1 hybrids and their parents. Consistent with the results of previous studies [8,31,43], we suggest that the enriched metabolism-related pathways identified in this study may directly contribute to growth heterosis in hybrid tilapia.

4.3. Analysis of Candidate DEGs Involved in Ribosome Biosynthesis in Eukaryotes

Ribosome biogenesis and protein synthesis are fundamental rate-limiting steps for cell growth and proliferation [44]. In eukaryotes, ribosome assembly is a rate-limiting step in ribosomal biogenesis. Ribosomal biogenesis is an elaborate process that determines the rate of protein synthesis, and by controlling a main anabolic cellular process, it regulates accumulation of cellular mass or cell growth [45]. Here, many key enzymes for eukaryotic ribosome biosynthesis in hybrid tilapia, *SNU13*, *DKC1*, *Nug1/2*, *MPP10*, *UTP4*, *UTP5*, *UTP14*, *UTP10*, and *UTP15*, were significantly decreased compared with their parents, which is consistent with the findings of Xiao et al. [7] on the domestic silkworm. Xie et al. [42] showed that the fast-growth phenotype of the ark shell *Scapharca kagoshimensis* may be attributed to lower energy requirements for metabolism maintenance, and more efficient protein biosynthesis and degradation. These findings revealed that efficiency of protein metabolism plays a role in growth heterosis in hybrid tilapia.

4.4. Analysis of Candidate DEGs Involved in Basal Defense Response

GSH-Px is an important peroxidase that belongs to the antioxidant defense system, which plays a fundamental role in overall defense mechanisms and strategies of organisms [46]. It was speculated that individuals with lower *GSH-Px* activity are susceptible to antioxidant protection [47]. HSPs are highly conserved molecular chaperones associated with helping other proteins fold properly during synthesis or repair of misassembled proteins [48]. HSPs, some defense genes and immune genes were significantly down-regulated in the largest individual sea cucumbers compared with the smallest ones [20]. In the current study, GSH-Px and HSPs (HSPA5 and HSP70) were significantly down-regulated in hybrid tilapia compared with their parents, indicating that its basal defense response was repressed. *Pseudomonas syringae* infection of *Arabidopsis* F_1 hybrids demonstrated that the reductions in basal defense gene activity in these hybrids does not necessarily compromise their ability to mount a defense response comparable to the parents [49]. Consistent with the results of previous studies [50,51], the repressed expression of basal defense response may promote growth in hybrid tilapia.

5. Conclusions

Hybrid tilapia exhibited higher growth rates than their parents, *O. niloticus* and *O. aureus*. Here, we provide a global view of the transcriptomic divergence of hybrid tilapia and their parental lines using RNA-Seq. A total of 2319 DEGs were identified. Trend co-expression analysis revealed that non-additive expression was prominent in hybrid tilapia compared with their parents. Interestingly, the metabolic pathway was more highly regulated in fatty acid metabolism and carbon metabolism, whereas ribosome biosynthesis in eukaryotes and basal defense response were significantly down-regulated. These findings provide new insights into our understanding of growth heterosis in hybrid tilapia.

Supplementary Materials: The following are available online at https://www.mdpi.com/article/10.3390/fishes7010043/s1. Figure S1: DEGs analysis and volcano plot for "NA vs. N", "NA vs. A", and "N vs. A". The *x*-axis is the value of Log2 (Fold Change), and the *y*-axis is the value of -Log_{10} (FDR). The red dots reveal the up-regulated DEGs, the green dots reveal the down-regulated DEGs, and black dots reveal non-differentially expressed genes. NA, N, and A denote hybrid tilapia, *O. niloticus*, and *O. aureus*, respectively. Figure S2: GO annotation of significantly up-regulated DEGs between *O. niloticus* or *O. aureus* and hybrid tilapia. Figure S3: GO annotation of significantly down-regulated DEGs between *O. niloticus* or *O. aureus* and hybrid tilapia. Table S1. Summary statistics of clean transcriptome sequencing data. Table S2. Sequencing data and selected reference genome sequence alignment results.

Author Contributions: Conceptualization, J.Z. and Z.Z.; methodology, J.Z. and D.L.; software, B.C.; validation, J.Z. and W.X.; formal analysis, J.Y.; investigation, J.Z. and D.L.; resources, D.L.; data curation, J.Z. and Z.Z.; writing—original draft preparation, J.Z.; writing—review and editing, J.Z.; visualization, J.Z. and D.L.; supervision, J.Y.; project administration, L.X.; funding acquisition, L.X. and H.Y. All authors have read and agreed to the published version of the manuscript.

Funding: This research was funded by Central Public-Interest Scientific Institution Basal Research Fund, Freshwater Fisheries Research Center, CAFS, grant number 2021JBFM04; China Agriculture Research System of MOF and MARA, grant number CARS-46 and Central Public-Interest Scientific Institution Basal Research Fund, CAFS, grant number 2020TD37.

Institutional Review Board Statement: The study was conducted according to the guidelines of the Declaration of Helsinki, and approved by the ethics committee of laboratory animal welfare and ethics of Freshwater Fisheries Research Center, Chinese Academy of Fishery Sciences (CAFS), project identification code: CARS-46. All animal procedures were performed according to the Zhejiang Laboratory Animal Management guidelines (000014349/2017-768264) on the Use and Care of Animals.

Data Availability Statement: All raw reads in the present study are archived in the National Center for Biotechnology Information (NCBI) Short Read Archive (SRA) databases under BioProject PRJNA792260(SUB10844155), with the accession numbers SRR17399951, SRR17399952 and SRR17399953.

Acknowledgments: We thank Mallory Eckstut for editing the English text of a draft of this manuscript. We also thank Chengliang Wei from the Freshwater Fisheries Research Center, CAFS for his contribution to the tilapia culture.

Conflicts of Interest: The authors declare no conflict of interest.

References

1. Yang, H.; Li, Q. The DNA methylation level is associated with the superior growth of the hybrid crosses in the Pacific oyster *Crassostrea gigas*. *Aquaculture* **2022**, *547*, 737421. [CrossRef]
2. Wang, S.; Tang, C.; Tao, M.; Qin, Q.; Zhang, C.; Luo, K.; Zhao, R.; Wang, J.; Ren, L.; Xiao, J.; et al. Establishment and application of distant hybridization technology in fish. *Sci. China Life Sci.* **2019**, *62*, 22–45. [CrossRef] [PubMed]
3. Li, S.; Zhou, Y.; Yang, C.; Fan, S.; Huang, L.; Zhou, T.; Wang, Q.; Zhao, R.; Tang, C.; Tao, M.; et al. Comparative analyses of hypothalamus transcriptomes reveal fertility-, growth-, and immune-related genes and signal pathways in different ploidy cyprinid fish. *Genomics* **2021**, *113*, 595–605. [CrossRef] [PubMed]
4. Jiang, G.; Li, Q.; Xu, C.; Liu, S.; Kong, L.; Yu, H. Reciprocal hybrids derived from *Crassostrea gigas* and *C. angulata* exhibit high heterosis in growth, survival and thermos tolerance in northern China. *Aquaculture* **2021**, *545*, 737173. [CrossRef]
5. Meng, L.; Li, Q.; Xu, C.; Liu, S.; Kong, L.; Yu, H. Hybridization improved stress resistance in the Pacific oyster: Evidence from physiological and immune responses. *Aquaculture* **2021**, *545*, 737227. [CrossRef]
6. Xing, Q.; Yang, Z.; Zhu, X.; Liu, J.; Huang, X.; Hu, J.; Bao, Z. Interspecific hybridization between *Patinopecten yessoensis* (♀) and *P. caurinus* (♂) with heterosis in growth and temperature tolerance. *Aquaculture* **2022**, *547*, 737489. [CrossRef]
7. Xiao, R.; Yuan, Y.; Zhu, F.; He, S.; Ge, Q.; Wang, X.; Taha, R.; Chen, K. Transcriptomics and proteomics-based analysis of heterosis on main economic traits of silkworm, *Bombyx Mori*. *J. Proteomics* **2020**, *229*, 103941. [CrossRef]
8. Zhang, G.; Li, J.; Zhang, J.; Liang, X.; Zhang, X.; Wang, T.; Yin, S. Integrated analysis of transcriptomic, miRNA and proteomic changes of a novel hybrid yellow catfish uncovers key roles for miRNAs in heterosis. *Mol. Cell. Proteomics* **2019**, *18*, 1437–1453. [CrossRef]
9. Zhong, H.; Zhou, Y.; Zhang, H.; Xiao, W. DNA methylation pattern is associated with elevated expression of DGAT2 in hybrid tilapia. *Aquacult. Nutr.* **2021**, *27*, 1750–1760. [CrossRef]

10. Sun, Y.; Guo, C.; Wang, D.; Li, X.F.; Xiao, L.; Zhang, X.; You, X.; Shi, Q.; Hu, G.; Fang, C.; et al. Transcriptome analysis reveals the molecular mechanisms underlying growth superiority in a novel grouper hybrid (*Epinephelus fuscogutatus* ♀× *E. lanceolatus* ♂). *BMC Genet.* **2016**, *17*, 24. [CrossRef]
11. Sun, Y.; Huang, Y.; Hu, G.; Zhang, X.; Ruan, Z.; Zhao, X.; Guo, C.; Tang, Z.; Li, X.; You, X.; et al. Comparative Transcriptomic study of muscle provides new insights into the growth superiority of a novel grouper hybrid. *PLoS ONE* **2016**, *11*, e168802. [CrossRef]
12. Gao, F.; Lu, W.; Shi, Y.; Zhu, H.; Wang, Y.; Tu, H.; Gao, Y.; Zhou, L.; Gui, J.; Zhao, Z. Transcriptome profiling revealed the growth superiority of hybrid pufferfish derived from *Takifugu obscurus* ♀× *Takifugu rubripes* ♂. *Comp. Biochem. Physiol. Genom. Proteomics* **2021**, *40*, 100912. [CrossRef] [PubMed]
13. Gomes, F.; Watanabe, L.; Vianez, J.; Nunes, M.; Cardoso, J.; Lima, C.; Schneider, H.; Sampaio, I. Comparative analysis of the transcriptome of the Amazonian fish species *Colossoma macropomum* (tambaqui) and hybrid tambacu by next generation sequencing. *PLoS ONE* **2019**, *14*, e212755. [CrossRef] [PubMed]
14. Zhou, Y.; Zhang, X.; Xu, Q.; Yan, J.; Yu, F.; Wang, F.; Xiao, J.; Luo, Y.; Zhong, H. Nonadditive and allele-specific expression of insulin-like growth factor 1 in Nile tilapia (*Oreochromis niloticus*, ♀) × blue tilapia (*O. aureus*, ♂) hybrids. *Comp. Biochem. Physiol. Part B Biochem. Mol. Biol.* **2019**, *232*, 93–100. [CrossRef]
15. Zhong, H.; Zhang, X.; Xu, Q.; Yan, J.; Han, Z.; Zheng, H.; Xiao, J.; Tang, Z.; Wang, F.; Luo, Y.; et al. Nonadditive and asymmetric allelic expression of growth hormone in hybrid tilapia. *Front. Genet.* **2019**, *10*, 961. [CrossRef] [PubMed]
16. Wang, J.; Lamer, J.T.; Gaughan, S.; Wachholtz, M.; Wang, C.; Lu, G. Transcriptomic comparison of invasive bigheaded carps (*Hypophthalmichthys nobilis* and *Hypophthalmichthys molitrix*) and their hybrids. *Ecol. Evol.* **2016**, *6*, 8452–8459. [CrossRef]
17. Chen, S.; Zhang, Z.; Ji, H.; Xu, S.; Yang, Y.; Jia, C.; Zhu, F.; Meng, Q.; Sun, R.; Zhang, Z.; et al. Transcriptome profiles of F1 hybrids (*Acanthopagrus schlegelii* ♂× *Pagrus major* ♀) and parents reveal hybrid effects on individual development. *Aquac. Res.* **2020**, *51*, 4011–4021. [CrossRef]
18. Zheng, G.; Wu, C.; Liu, J.; Chen, J.; Zou, S. Transcriptome analysis provides new insights into the growth superiority of a novel backcross variety, *Megalobrama amblycephala* ♀× (*M. amblycephala* ♀× *Culter alburnus* ♂). *Aquaculture* **2019**, *512*, 734317. [CrossRef]
19. Zhang, H.; Xu, X.; He, Z.; Zheng, T.; Shao, J. De novo transcriptome analysis reveals insights into different mechanisms of growth and immunity in a Chinese soft-shelled turtle hybrid and the parental varieties. *Gene* **2017**, *605*, 54–62. [CrossRef]
20. Gao, K.; Wang, Z.; Qiu, X.; Song, J.; Wang, H.; Zhao, C.; Wang, X.; Chang, Y. Transcriptome analysis of body wall reveals growth difference between the largest and smallest individuals in the pure and hybrid populations of *Apostichopus japonicus*. *Comp. Biochem. Physiol. Part D Genom. Proteom.* **2019**, *31*, 100591. [CrossRef] [PubMed]
21. Xiao, Q.; Huang, Z.; Shen, Y.; Gan, Y.; Wang, Y.; Gong, S.; Lu, Y.; Luo, X.; You, W.; Ke, C. Transcriptome analysis reveals the molecular mechanisms of heterosis on thermal resistance in hybrid abalone. *BMC Genom.* **2021**, *22*, 650. [CrossRef]
22. Bureau of Fisheries; Ministry of Agriculture and Rural Affairs; National Fisheries Technology Extension Center; China Society of Fisheries. *2020 China Fishery Statistical Yearbook*; China Agriculture Press: Beijing, China, 2021; p. 25.
23. Lago, A.D.A.; Rezende, T.T.; Dias, M.A.D.; Freitas, R.T.F.D.; Hilsdorf, A.W.S. The development of genetically improved red tilapia lines through the backcross breeding of two *Oreochromis niloticus* strains. *Aquaculture* **2017**, *472*, 17–22. [CrossRef]
24. Bartie, K.L.; Taslima, K.; Bekaert, M.; Wehner, S.; Syaifudin, M.; Taggart, J.B.; de Verdal, H.; Rosario, W.; Muyalde, N.; Benzie, J.A.H.; et al. Species composition in the Molobicus hybrid tilapia strain. *Aquaculture* **2020**, *526*, 735433. [CrossRef]
25. Parrino, V.; Cappello, T.; Costa, G.; Cannavà, C.; Sanfilippo, M.; Fazio, F.; Fasulo, S. Comparative study of haematology of two teleost fish (*Mugil cephalus* and *Carassius auratus*) from different environments and feeding habits. *Eur. Zool. J.* **2018**, *85*, 193–199. [CrossRef]
26. Parrino, V.; De Marco, G.; Minutoli, R.; Lo Paro, G.; Giannetto, A.; Cappello, T.; De Plano, L.M.; Cecchini, S.; Fazio, F. Effects of pesticides on *Chelon labrosus* (Risso, 1827) evaluated by enzymatic activities along the north eastern Sicilian coastlines (Italy). *Eur. Zool. J.* **2021**, *88*, 540–548. [CrossRef]
27. Schnable, P.S.; Springer, N.M. Progress toward understanding heterosis in crop plants. *Annu. Rev. Plant Biol.* **2013**, *64*, 71–88. [CrossRef] [PubMed]
28. Han, Z.; Li, Q.; Liu, S.; Kong, L. Crossbreeding of three different shell color lines in the Pacific oyster reveals high heterosis for survival but low heterosis for growth. *Aquaculture* **2020**, *529*, 735621. [CrossRef]
29. Gu, H.; Qi, X.; Jia, Y.; Zhang, Z.; Nie, C.; Li, X.; Li, J.; Jiang, Z.; Wang, Q.; Qu, L. Inheritance patterns of the transcriptome in hybrid chickens and their parents revealed by expression analysis. *Sci. Rep.* **2019**, *9*, 5750. [CrossRef]
30. Yang, J.; Luo, S.; Li, J.; Zheng, Z.; Du, X.; Deng, Y. Transcriptome analysis of growth heterosis in pearl oyster *Pinctada fucata* martensii. *FEBS Open Bio* **2018**, *8*, 1794–1803. [CrossRef]
31. Liang, S.; You, W.; Luo, X.; Ke, J.; Huang, M.; Guo, Y.; Ke, C. Integrated analysis of mRNA and miRNA changes in two *Haliotis diversicolor* genotypes and their hybrid. *Front. Mar. Sci.* **2021**, *8*, 667636. [CrossRef]
32. Kim, D.; Pertea, G.; Trapnell, C.; Pimentel, H.; Kelley, R.; Salzberg, S.L. TopHat2: Accurate alignment of transcriptomes in the presence of insertions, deletions and gene fusions. *Genome Biol.* **2013**, *14*, R36. [CrossRef] [PubMed]
33. Leng, N.; Dawson, J.A.; Thomson, J.A.; Ruotti, V.; Rissman, A.I.; Smits, B.M.; Haag, J.D.; Gould, M.N.; Stewart, R.M.; Kendziorski, C. EBSeq: An empirical Bayes hierarchical model for inference in RNA-seq experiments. *Bioinformatics* **2013**, *29*, 1035–1043. [CrossRef] [PubMed]
34. Young, M.D.; Wakefield, M.J.; Smyth, G.K.; Oshlack, A. Gene ontology analysis for RNA-seq: Accounting for selection bias. *Genome Biol.* **2010**, *11*, R14. [CrossRef] [PubMed]

35. Xie, C.; Mao, X.; Huang, J.; Ding, Y.; Wu, J.; Dong, S.; Kong, L.; Gao, G.; Li, C.Y.; Wei, L. KOBAS 2.0: A web server for annotation and identification of enriched pathways and diseases. *Nucleic Acids Res.* **2011**, *39*, W316–W322. [CrossRef]
36. Livak, K.J.; Schmittgen, T.D. Analysis of relative gene expression data using real-time quantitative PCR and the 2(-Delta Delta C(T)) Method. *Methods* **2001**, *25*, 402–408. [CrossRef]
37. Paiva, P.; Medina, F.E.; Viegas, M.; Ferreira, P.; Neves, R.; Sousa, J.; Ramos, M.J.; Fernandes, P.A. Animal fatty acid synthase: A chemical nanofactory. *Chem. Rev.* **2021**, *121*, 9502–9553. [CrossRef]
38. Soo, H.J.; Sam, K.K.; Chong, J.; Lau, N.S.; Ting, S.Y.; Kuah, M.K.; Kwang, S.Y.; Ranjani, M.; Shu-Chien, A.C. Functional characterisation of fatty acyl desaturase, Fads2, and elongase, Elovl5, in the Boddart's goggle-eyed goby *Boleophthalmus boddarti* (Gobiidae) suggests an incapacity for long-chain polyunsaturated fatty acid biosynthesis. *J. Fish Biol.* **2020**, *97*, 83–99. [CrossRef]
39. Fothergill-Gilmore, L.A.; Michels, P.A. Evolution of glycolysis. *Prog. Biophys. Mol. Biol.* **1993**, *59*, 105–235. [CrossRef]
40. Xiong, Y.; Lei, Q.Y.; Zhao, S.; Guan, K.L. Regulation of glycolysis and gluconeogenesis by acetylation of PKM and PEPCK. *Cold Spring Harb. Symp. Quant. Biol.* **2012**, *76*, 285–289. [CrossRef]
41. Polakof, S.; Panserat, S.; Soengas, J.L.; Moon, T.W. Glucose metabolism in fish: A review. *J. Comp. Physiol. B* **2012**, *182*, 1015–1045. [CrossRef]
42. Xie, X.; Teng, W.; Sun, X.; Liang, M.; Du, S.; Zhu, S.; Liu, X.; Nie, H.; Wang, Q. Transcriptomic analysis of the ark shell *Scapharca kagoshimensis*: De novo assembly and identification of genes and pathways involved growth. *Aquac. Rep.* **2020**, *18*, 100522. [CrossRef]
43. Wang, Z.; Cui, J.; Song, J.; Wang, H.; Gao, K.; Qiu, X.; Gou, M.; Li, X.; Hu, Z.; Wang, X.; et al. Comparative transcriptome analysis reveals growth-related genes in juvenile Chinese sea cucumber, Russian sea cucumber, and their hybrids. *Mar. Biotechnol.* **2018**, *20*, 193–205. [CrossRef] [PubMed]
44. Kang, J.; Brajanovski, N.; Chan, K.T.; Xuan, J.; Pearson, R.B.; Sanij, E. Ribosomal proteins and human diseases: Molecular mechanisms and targeted therapy. *Signal Transduct. Target. Ther.* **2021**, *6*, 323. [CrossRef] [PubMed]
45. Abetov, D.A.; Kiyan, V.S.; Zhylkibayev, A.A.; Sarbassova, D.A.; Alybayev, S.D.; Spooner, E.; Song, M.S.; Bersimbaev, R.I.; Sarbassov, D.D. Formation of mammalian preribosomes proceeds from intermediate to composed state during ribosome maturation. *J. Biol. Chem.* **2019**, *294*, 10746–10757. [CrossRef] [PubMed]
46. Ighodaro, O.M.; Akinloye, O.A. First line defence antioxidants-superoxide dismutase (SOD), catalase (CAT) and glutathione peroxidase (GPX): Their fundamental role in the entire antioxidant defence grid. *Alex. J. Med.* **2018**, *54*, 287–293. [CrossRef]
47. Chabory, E.; Damon, C.; Lenoir, A.; Kauselmann, G.; Kern, H.; Zevnik, B.; Garrel, C.; Saez, F.; Cadet, R.; Henry-Berger, J.; et al. Epididymis seleno-independent glutathione peroxidase 5 maintains sperm DNA integrity in mice. *J. Clin. Investig.* **2009**, *119*, 2074–2085. [CrossRef] [PubMed]
48. Pham, T.H.; Cheng, T.C.; Wang, P.C.; Chen, S.C. Protective efficacy of four heat-shock proteins as recombinant vaccines against photobacteriosis in Asian seabass (*Lates calcarifer*). *Fish Shellfish Immunol.* **2021**, *111*, 179–188. [CrossRef]
49. Groszmann, M.; Gonzalez-Bayon, R.; Lyons, R.L.; Greaves, I.K.; Kazan, K.; Peacock, W.J.; Dennis, E.S. Hormone-regulated defense and stress response networks contribute to heterosis in *Arabidopsis* F1 hybrids. *Proc. Natl. Acad. Sci. USA* **2015**, *112*, E6397–E6406. [CrossRef]
50. Miller, M.; Song, Q.; Shi, X.; Juenger, T.E.; Chen, Z.J. Natural variation in timing of stress-responsive gene expression predicts heterosis in intraspecific hybrids of Arabidopsis. *Nat. Commun.* **2015**, *6*, 8453. [CrossRef]
51. Gonzalez-Bayon, R.; Shen, Y.; Groszmann, M.; Zhu, A.; Wang, A.; Allu, A.D.; Dennis, E.S.; Peacock, W.J.; Greaves, I.K. Senescence and defense pathways contribute to heterosis. *Plant Physiol.* **2019**, *180*, 240–252. [CrossRef]